Pergamon

Int. J. Solids Structures Vol. 35, Nos 28–29, pp. 3717–3735, 1998

0020–7683/98 $19.00 + .00

PII: S0020–7683(97)00234–5

ANTI-SYMMETRIC ANGLE-PLY LAMINATED THICK CYLINDRICAL PANELS

H. R. H. KABIR*
Department of Civil Engineering, Kuwait University P.O. Box 5969, Safat 13060, Kuwait

(*Received* 4 *January* 1997; *in revised form* 20 *June* 1997)

Abstract—Hither-to-fore an unavailable analytical solution (strong form or differential form) to the boundary-value problem of advanced fiber reinforced anti-symmetric angle-ply laminated cylindrical panels of rectangular planform subjected to static loadings is presented. A variationally consistent higher shell theory is utilized that generates five highly coupled fourth order partial differential equations in five unknowns, three displacements, and two rotations. A boundary continuous double Fourier series-based solution functions is assumed to solve such equations in conjunction with the admissible boundary conditions. The numerical results constitute the study of convergence of displacements, in-plane forces, and moments; and spatial variations of them presented in the form of contour plotting for various parametric effects. These, hither-to unavailable solutions, and analytically obtained numerical results should serve as bench-marks for future comparisons of popular approximate methods (integral form or weak form), such as finite element, boundary element, finite difference, Galerkin approach, Rayleigh–Ritz, collocation, least-squares methods, and experimental results, etc.

INTRODUCTION

The shell theory is a transition from the three-dimensional structural behavior to the two-dimensional domain characteristics. This theory is employed with an assumption that the through-thickness variation is not a dominating factor in comparison to the spatial variations and their magnitudes. The outcome was the development of the thin shell theory, the first of its kind, as established by Love and Kirchhoff (Ambartsumyan, 1953; Donnell, 1933; Flugge, 1960; Greenberg and Stavsky, 1980; Seide, 1975; McElman, 1971; Jones and Morgan, 1975; Soldatos and Tzivanididis, 1982; Soldatos, 1984) a century ago. Later, the industry has realized that if the thickness of the shell increases, structural responses are not in a good agreement with the reality in general, and particularly along the thickness direction. A theory known as the Reissner and Mindlin shear deformation theory (RMSDT) (Bert and Reddy, 1982; Bert and Kumar 1982; Stavsky and Lowey, 1971; Reissner, 1944; Mindlin, 1951; Chaudhuri, 1989; Librescu *et al.*, 1989; Kabir and Chaudhuri, 1994) has come forward to subdue the frustration of industries. This theory considers the effect of thickness in the form recognizing the contribution of transverse shear deformations (TSD) along the thickness. The through-thickness variations are assumed constant, a deviation from the reality as TSD vanishes at the top and bottom surfaces. However, this theory, to some extent (say, for span-to-thickness ratios = 20 to 40) provides reasonable results in a moderately thick situation. As the shell thickness further increases, due to the industries' demands, the response of the later theory appears to be inaccurate. A new shell theory has emerged very recently that considers the short comings of RMSDT, known as higher order shear deformation theory (HOSDT). The development, faultiness, short comings, and accuracy of this theory in the sense of through-thickness behavior are available, e.g., in Lo *et al.* (1977a,b), Nelson and Lorch (1974), Levinson (1980), Murthy (1989), Reddy and Liu (1985), Librescu *et al.* (1989), etc. All the aforementioned theories belong to the equivalent single layer theory, and are very popular in determining the global response of the structures. For the case of advanced fiber reinforced (e.g., graphite/epoxy, boron/epoxy,

* Tel.: 00-965-481-1188. Fax: 00-956-481-7524. E-mail: humayun@kuc01.kuniv.edu.kw.

Kevlar/epoxy, graphite/PEEK, etc.) laminated plates and shells, due to the low transverse shear rigidities, the HOSDT works very efficiently (Reddy and Robbins, 1994).

As the through-thickness theory is ameliorated for the shell structures, its corresponding analytical solutions (strong from) become more arduous, if not impossible. In the domains of HOSDT, for the case of laminated shells or panels, analytical solutions to the boundary value problems are limited to few boundary conditions, laminations, and solution techniques. For example, pioneers Reddy and Liu (1985) have presented a HOSDT-based analysis for shallow cross-ply doubly-curved panels of rectangular planform, with the SS3 type (according to the classification of Hoff and Rehfield, 1965) simply supported boundary conditions prescribed at all edges. They have used the Navier approach in their analysis formulation. Recently, Librescu *et al.* (1989) have presented HOSDT-based analytical solutions to shallow cross-ply laminated doubly-curved shells and cylindrical panels with various boundary conditions using the Levy-type approach. This approach has constrained them selecting boundary conditions of two opposite edges as of SS3-type simply supported, while the other edges are combinations of remaining boundary conditions (e.g., SS1, SS2, SS3, C1, C2, C3, or C4).

To the best of the knowledge of the author, no analytical solutions other than the cross-ply laminations, and aforementioned boundary conditions are reported in the literature for cylindrical panels. It may be mentioned here that one may obtain solutions of any lamination sequences and boundary conditions of cylindrical panels using approximate techniques, such as finite element, Galerkin, etc. However, approximate solution techniques (weak form or integral form) and exact solution techniques (differential or strong form) are fundamentally different, as they seek solutions in different function spaces. A stronger solution requires square integrable functions, and its first and second derivatives within the domain boundary, a severe restriction in comparison to the weak form of solution where the last two restrictions as of the stronger form are not obligatory. As a result, functions or solution procedures that assuage the stronger conditions are not much conspicuous in the literature. It is a norm in the realm of boundary-value problems that the solution functions or the techniques that are suitable in one boundary-value problem may not be true to the other. In laminated shell boundary value problems, a change in lamination sequences, angles, and stacking patterns always bring forth a new frontier of challenge for the researchers.

An extensive literature search has revealed that the analytical solution (strong form or differential form) to the boundary value problem of a cylindrical panel with higher order shell theory of rectangular planform with anti-symmetric laminations has not yet been reported in the literature.

Therefore, the prime objective here is to develop an analytical solution to the boundary value problem of a cylindrical panel of rectangular planform with anti-symmetric laminations. For example, SS2-type simply supported boundary conditions at all edges is considered. The second objective is to study, numerically, the convergence, and the spatial variations of displacements, normal forces, and moments for various parametric effects. The last objective is to compare the present results with an available finite element solution, an approximate approach.

THEORETICAL FORMULATION

An orthogonal curvilinear coordinate system x_i $(i = 1, 2, 3)$ is selected to represent the geometry and deformation characteristics of a cylindrical panel of span $a \times b$ and radius r_{11} as shown in Fig. 1. The middle surface of the panel thickness is taken as the reference surface, and the coordinate system is placed on it with x_3 being normal. The total thickness of the panel is assumed as $h = \Sigma_{i=1}^{N} t_{\langle i \rangle}$, where $t_{\langle k \rangle}$ represents the thickness of the kth layer, and N denotes the total number of layers. The strain–displacement relations from the linear (small deformation) theory of elasticity in a curvilinear coordinate system are given as follows (Reddy and Liu, 1985):

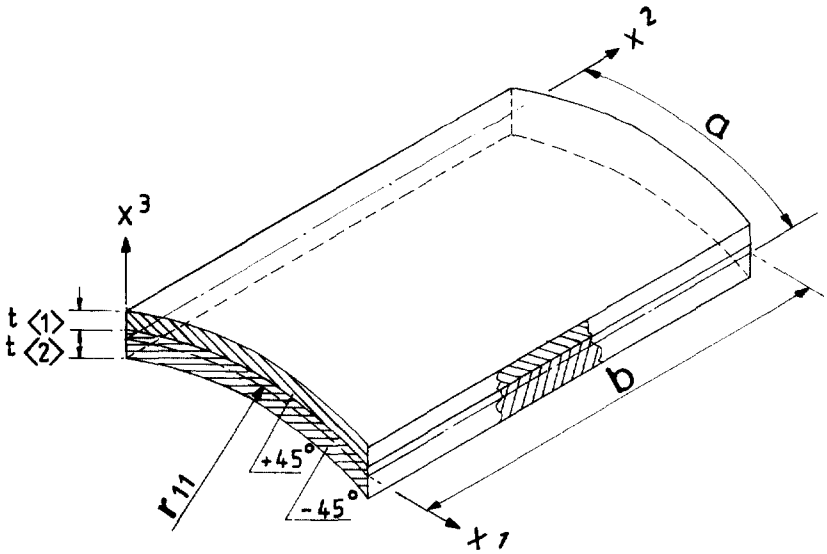

Fig. 1. A laminated cylindrical panel. u_3^*, M_1^*, and M_2^* N_1^* and N_2^*.

$$\varepsilon_1(x_1,x_2,x_3) = \frac{1}{\left[1+\left(\frac{x_3}{r_{11}}\right)\right]g_1}\left[\bar{u}_{1,1}+\frac{1}{g_2}g_{1,2}\bar{u}_2+\frac{g_1}{r_{11}}\bar{u}_3\right]$$

$$\varepsilon_2(x_1,x_2,x_3) = [\bar{u}_{2,2}]$$

$$\varepsilon_3(x_1,x_2,x_3) = \bar{u}_{3,3}$$

$$\varepsilon_4(x_1,x_2,x_3) = \bar{u}_{3,2}+\bar{u}_{2,3}$$

$$\varepsilon_5(x_1,x_2,x_3) = \frac{1}{\left[1+\left(\frac{x_3}{r_{11}}\right)\right]g_1}\left[\bar{u}_{3,1}-\frac{1}{r_{11}}g_1\bar{u}_1\right]+\bar{u}_{1,3}$$

$$\varepsilon_6(x_1,x_2,x_3) = \frac{1}{\left[1+\left(\frac{x_3}{r_{11}}\right)\right]g_1}\bar{u}_{2,1}+\bar{u}_{1,2} \qquad \text{(1a–f)}$$

where $\bar{u}_i$ $(i = 1,2,3)$ and ε_i $(i = 1,\ldots,6)$ represent displacement vector and strain vector, respectively, at any point on a parallel surface. g_1 and g_2 are the first fundamental quantities of the shell reference surface. For the variationally higher order shell theory, $\bar{u}_i$ $(i = 1,2,)$ are considered as of the form (Reddy and Liu, 1985):

$$\bar{u}_1 = \left(1+\frac{x_3}{r_{11}}\right)u_1+x_3\varphi_1-x_3^3\frac{4}{3h^2}\left[\varphi_1+\frac{1}{g_1}u_{3,1}\right]$$

$$\bar{u}_2 = u_2+x_3\varphi_2-x_3^3\frac{4}{3h^2}\varphi_2$$

$$\bar{u}_3 = u_3 \qquad \text{(2a–c)}$$

where u_i are displacements at the midsurface of the shell. The components φ_1 and φ_2 are rotations of normal about x_2 and x_1 axes, respectively. Introduction of eqns (2) into eqns (1) supplies the following strain–displacement relations (Reddy and Liu, 1985):

$$\varepsilon_1 = \varepsilon_1^0 + x_3(\kappa_1^0 + x_3^2\kappa_1^2)$$

$$\varepsilon_2 = \varepsilon_2^0 + x_3(\kappa_2^0 + x_3^2\kappa_2^2)$$

$$\varepsilon_4 = \varepsilon_4^0 + x_3^2\kappa_4^1$$

$$\varepsilon_5 = \varepsilon_5^0 + x_3^2\kappa_5^1$$

$$\varepsilon_6 = \varepsilon_6^0 + x_3(\kappa_6^0 + x_3^2\kappa_6^2) \tag{3a–e}$$

where

$$\varepsilon_1^0 = u_{1,1} + \frac{u_3}{r_{11}}; \quad \kappa_1^0 = \varphi_{1,1}; \quad \kappa_1^2 = -\frac{4}{3h^2}(\varphi_{1,1} + u_{3,11}); \quad \varepsilon_2^0 = u_{2,2}; \quad \kappa_2^0 = \varphi_{2,2}$$

$$\kappa_2^2 = -\frac{4}{3h^2}(\varphi_{2,2} + u_{3,22}); \quad \varepsilon_4^0 = \varphi_2 + u_{3,2}; \quad \kappa_4^1 = -\frac{4}{3h^2}(\varphi_2 + u_{3,2})$$

$$\varepsilon_5^0 = \varphi_1 + u_{3,1}; \quad \kappa_5^1 = -\frac{4}{3h^2}(\varphi_1 + u_{3,1}); \quad \varepsilon_6^0 = u_{2,1} + u_{1,2}$$

$$\kappa_6^0 = \varphi_{2,1} + \varphi_{1,2}; \quad \kappa_6^2 = -\frac{4}{3h^2}(\varphi_{2,1} + \varphi_{1,2} + 2u_{3,12}) \tag{4a–m}$$

The governing partial differential equations derived using the principle of virtual work are

$$N_{1,1} + N_{6,2} = 0, \qquad N_{6,1} + N_{2,2} = 0$$

$$Q_{1,1} + Q_{2,2} - \frac{4}{3h^2}(K_{1,1} + K_{2,2}) + \frac{4}{3h_2}(P_{1,11} + P_{2,22} + 2P_{6,12}) - \frac{N_1}{r_{11}} + q = 0$$

$$M_{1,1} + M_{6,2} - Q_1 + \frac{4}{h^2}K_1 - \frac{4}{h^2}(P_{1,1} + P_{6,2}) = 0$$

$$M_{6,1} + M_{2,2} - Q_2 + \frac{4}{h^2}K_2 - \frac{4}{h^2}(P_{6,1} + P_{2,2}) = 0 \tag{5a–e}$$

where N_i, M_i, and P_i are stress resultants, stress couples, and second moment of stress couples, respectively. q denotes a uniformly distributed transverse load. Q_i represent transverse shear stress resultants, and K_i denote second moment of Q_i.

The resultants of in-plane stress, stress couples, inertia of stress couples, and transverse shear stress, respectively, are defined as

$$\begin{Bmatrix} N_{\alpha\beta} \\ M_{\alpha\beta} \\ P_{\alpha\beta} \\ Q_{\alpha 3} \\ K_{\alpha 3} \end{Bmatrix} = \sum_{K=1}^{N} \int_{t_{\langle k-1\rangle}}^{t_{\langle k\rangle}} \begin{Bmatrix} \sigma_{\langle k\rangle}^{\alpha\beta} \\ \sigma_{\langle k\rangle}^{\alpha\beta} x_3 \\ \sigma_{\langle k\rangle}^{\alpha\beta}(x_3) \\ \sigma_{\langle k\rangle}^{\alpha 3} \\ \sigma_{\langle k\rangle}^{\alpha 3} x_3^2 \end{Bmatrix} \mathrm{d}x^3 \tag{6}$$

where $N_{\alpha\alpha} = N_1$, $N_{\beta\beta} = N_2$, etc. The constitutive relation of each laminate is considered to be of the following form

$$\sigma^{\alpha\beta}_{(k)} = \left(E^{\alpha\beta\gamma\eta}_{(k)} - \frac{E^{\alpha\beta 33}_{(k)} E^{33\gamma\eta}_{(k)}}{E^{3333}_{(k)}} \right) e^{(k)}_{\gamma\eta} \tag{7}$$

$$\sigma^{a3}_{(k)} = 2E^{\alpha 3\gamma 3}_{(k)} e^{(k)}_{\gamma 3} \tag{8}$$

where $\sigma^{\alpha\beta}_{(k)}$ and $E^{\alpha\beta\gamma\eta}_{(k)}$ are stress and elastic moduli tensors, respectively, for a lamina; and $e^{(k)}_{\alpha\beta}$ represent the strain tensor of each lamina.

Finally, equilibrium eqns (5) can be expressed in the form of partial differential equations for cylindrical panels in terms of displacements and its derivatives, as shown below, in the most general form with constant coefficients:

$$a^i_j u_j + b^i_{jk} u_{j,k} + c^i_{jkl} u_{j,kl} + d^i_{jklm} u_{j,klm} + e^i_{jklmn} u_{j,klmn} = q_i \quad (i = 1, \ldots, 5) \tag{9}$$

where a^i_j, b^i_{jk}, c^i_{jkl}, d^i_{jklm}, and e^i_{jklmn} are constant coefficients, arising due to the lamination sequences, as defined in Appendix 1.

The above eqs (9) are highly coupled. The objective is to solve the above equations in conjunction with the admissible boundary conditions. The constrains that are imposed at the boundaries are of highly mixed type, in contrast to Dirichlet-, Neumann-, and Robin-types (Andrews, 1986). In the Dirichlet, and Neumann types, the functions, and their normal derivatives, respectively, are prescribed at the boundaries, while, in the Robin type, the functions as well as their normal derivatives simultaneously are assumed vanished at the boundaries. However, for the mixed type boundary conditions, functions, and their normal and tangential derivatives are set equal to zero at the boundaries. These pose a considerable amount of difficulties finding suitable solution functions and methodology in the domain of differential form of solutions. The following boundary conditions are selected.

(a) Dirichlet type:

$$\begin{aligned} u_1 = u_3 = \varphi_2 = 0 \quad & \text{at } x_1 = (0, a) \\ u_2 = u_3 = \varphi_1 = 0 \quad & \text{at } x_2 = (0, b) \end{aligned} \tag{10a,b}$$

(b) Mixed type:

$$\begin{aligned} N_6 = 0 \quad & \text{at all edges} \\ M_1 = P_1 = 0 \quad & \text{at } x_1 = (0, a) \\ M_2 = P_2 = 0 \quad & \text{at } x_2 = (0, b) \end{aligned} \tag{11a,b}$$

The above boundary conditions are known as SS2-type simply supported according to Hoff and Rehfield (1965).

Solution methodology

The solution functions for eqns (9) in conjunction with the prescribed boundary conditions are assumed in the following form:

$$u_1(x_1, x_2) = \sum_{m=1}^{\infty} \sum_{n=0}^{\infty} A_{mn}^{(1)} \sin(\alpha_m x_1) \cos(\beta_n x_2)$$

$$u_2(x_1, x_2) = \sum_{m=0}^{\infty} \sum_{n=1}^{\infty} A_{mn}^{(2)} \cos(\alpha_m x_1) \sin(\beta_n x_2)$$

$$u_3(x_1, x_2) = \sum_{m=1}^{\infty} \sum_{n=1}^{\infty} A_{mn}^{(3)} \sin(\alpha_m x_1) \sin(\beta_n x_2)$$

$$\varphi_1(x_1, x_2) = \sum_{m=0}^{\infty} \sum_{n=1}^{\infty} A_{mn}^{(4)} \cos(\alpha_m x_1) \sin(\beta_n x_2)$$

$$\varphi_2(x_1, x_2) = \sum_{m=1}^{\infty} \sum_{n=0}^{\infty} A_{mn}^{(5)} \sin(\alpha_m x_1) \cos(\beta_n x_2) \qquad (12a\text{–}e)$$

where $A_{mn}^{(j)}$ are Fourier constants. α_m and β_n are defined as $\pi m/a$ and $\pi n/b$, respectively. The assumed displacement functions [eqns (12a–e)] completely satisfy the Dirichlet boundary conditions at all edges. Therefore, obtaining first derivatives of the solution functions pose no difficulties. However, the complication arises for further differentiations in satisfying the mixed type boundary conditions due to the presence of ordinary discontinuities in the derivatives, before their introduction into the partial differential equations. The displacement function u_3 is considered to explain the above phenomena.

$$u_3 = \sum_{m=1}^{\infty} \sum_{n=0}^{\infty} A_{mn}^{(3)} \sin(\alpha_m x_1) \sin(\beta_n x_2) \quad 0 \leqslant x_1 \leqslant a; \quad 0 \leqslant x_2 \leqslant b \qquad (13)$$

$$u_{3,1} = \sum_{m=1}^{\infty} \sum_{n=1}^{\infty} \{\alpha_m A_{mn}^{(3)} \cos(\alpha_m x_1) \sin(\beta_n x_2)\} \quad 0 \leqslant x_1 \leqslant a; \quad 0 \leqslant x_2 \leqslant b \qquad (14)$$

$$u_{3,11} \sum_{m=1}^{\infty} \sum_{n=1}^{\infty} \{(\alpha_m)^2 A_{mn}^{(3)} \sin(\alpha_m x_1) \sin(\beta_n x_2)\} \quad 0 < x_1 < a; \quad 0 \leqslant x_2 \leqslant b \qquad (15)$$

Further differentiation of eqn (15) is not possible with respect to x_1 due to the discontinuities. In such an occasion eqn (15) is expanded in the following manner as suggested by Hobson (1926), Green (1944), Whitney (1970), Whitney and Leissa (1969), Chaudhuri (1989), and Kabir (1994):

$$u_{3,111} = \frac{1}{2} \sum_{n=1}^{\infty} g_{n(1)}^{3111} \sin(\beta_n x_2)$$

$$+ \sum_{m=1}^{\infty} \sum_{n=1}^{\infty} \{-(\alpha_m)^3 A_{mn}^{(1)} + \omega_m^{(1)} g_{n(1)}^{3111} + \omega_m^{(2)} g_{n(2)}^{3111}\} \cos(\alpha_m x_1) \sin(\beta_n x_2) \qquad (16)$$

where $\omega_m^{(1)}$ and $\omega_m^{(2)}$ are defined as

$$\begin{Bmatrix} \omega_i^{(1)} \\ \omega_i^{(2)} \end{Bmatrix} = \begin{Bmatrix} (0, 1) & \text{if } i \text{ is even} \\ (1, 0) & \text{if } i \text{ is odd} \end{Bmatrix} \qquad (17)$$

$g_{(1)}^{3111}$ and $g_{(2)}^{3111}$ are constants as defined in Appendix 3. This operation is applicable to all the situations where ordinary discontinuous exists in the derivatives. Finally, all the required derivatives can be introduced into eqns (9), as well as into the mixed boundary conditions (8). Expressing uniformly distributed transverse load $q_{\langle 0 \rangle}^3 = \Sigma_{m=1}^{\infty} \Sigma_{n=1}^{\infty} q_{mn}^3 \sin(\alpha_m x_1) \sin(\beta_n x_2)$, algebraic equations may be expressed as

$$\begin{bmatrix} K^i_{mn} + \sum_{\bar{n}=1}^{\infty}\sum_{\bar{m}=1}^{\infty} K^{i\_\_}_{mn} & C^i_{mn} + \sum_{\bar{n}=1}^{\infty}\sum_{\bar{m}=1}^{\infty} C^{i\_\_}_{mn} \\ {}_bK^i_{mn} + \sum_{\bar{n}=1}^{\infty}\sum_{\bar{m}=1}^{\infty} {}_bK^{i\_\_}_{mn} & {}_bC^i_{mn} + \sum_{\bar{n}=1}^{\infty}\sum_{\bar{m}=1}^{\infty} {}_bC^{i\_\_}_{mn} \end{bmatrix} \begin{Bmatrix} A^{(i)}_{mn} \\ g^{qrst}_{(1)\text{or}(2)} \end{Bmatrix} = \begin{Bmatrix} q^3_{mn} \\ 0 \end{Bmatrix} \tag{18}$$

where K^i_{mn} and C^i_{mn} are constant coefficients arising from eqns (9). ${}_bK^i_{mn}$ and ${}_bC^i_{mn}$ are constant coefficients arising from mixed type boundary conditions. $g^{qrst}_{(1)\text{or}(2)}$ are unknown constant coefficients due to the application of the situations as shown in eqn (16) for other derivatives. The double summation in eqn (18) is due to the expansion of the series functions as suggested by Kabir and Chaudhuri (1994, 1991).

A computer code AFSANA-ALTCP (A Fourier Series ANAlysis—Angle-ply Laminated Thick Cylindrical Panel) is developed in SUN workstation using FORTRAN-77 to solve the above mentioned equations.

NUMERICAL RESULTS AND DISCUSSIONS

The accuracy of a series solution is usually ascertained studying the convergence of the assumed solution functions, their derivatives, and mixture of functions and their first or second order derivatives (Robin-type). Spatial variations of them, in the form of contour plots, are always of interest, to study their behavior pointwise in the domain. The numerical results are presented for the following material properties characterizing each orthotropic lamina:

$$\frac{E_1}{E_2} = 25; \quad \frac{G_{12}}{E_2} = \frac{G_{13}}{E_2} = 0.5\frac{G_{23}}{E_2} = 0.2; \quad \nu_{12} = \nu_{13} = 0.25; \quad \nu_{23} = 0.49 \tag{19}$$

where E_1 and E_2 are Young moduli along major and minor axes, respectively, of the lamina. G_{12} is an in-plane shear modulus, while G_{13} and G_{23} are transverse shear moduli in x_1–x_3 and x_2–x_3 planes, respectively. ν_{ij} denote Poisson's ratios. A laminated cylindrical panel is generally marked using the order of the placement of lamina. For example, θ_1/θ_2 ($45^\circ/-45^\circ$ laminations in the present case) laminated panel refers to two layers of laminae having major material directions of top and bottom layers at an angle θ_1 (45°) and θ_2 (-45°), respectively, measured from projecting x_1-axis on to the shell surface, with rotation about x_3-axis using right hand rule. For the sake of convenience of presentation the following dimensionless quantities are defined.

$$u^*_3 = \frac{10^3 E_2 h^3 u_3}{qa^4}; \quad M^*_i = \frac{10^3 M_i}{qa^2} \quad (i = 1, 2); \quad N^*_i = \frac{10^3 N_i}{qa} \quad (i = 1, 2) \tag{20}$$

The normalized centrally measured transverse displacement u^*_3, moments M^*_1, and M^*_2 are plotted in Fig. 2, with respect to various values of $m = n$, for a cylindrical panel having radius-to-span ratio of 5, aspect ratio ($b/a = 1$) of 1, and span-to-thickness ratio of 10. A monotonic convergence has been observed in all the above cases. For the same cylindrical panel convergences of normalized centrally measured N^*_1, and N^*_2 are shown in Fig. 3, with minor oscillations observed at low $m = n$.

Figure 4 presents convergences of normalized centrally measured transverse displacement u^*_3, and moments M^*_1 and M^*_2 for a cylindrical panel with radius-to-span ratio of 5, aspect ratio of $b/a = 1$, and span-to-thickness ratio of 50, a relatively thin shell situation. The transverse displacement u^*_3 as expected converges very smoothly, while the moments (M^*_1, and M^*_2) show high oscillations at low $m = n$, and become smoother with the increase of $m = n$. For this cylindrical panel normalized centrally measured N^*_1, and N^*_2 show a convincing convergence as plotted in Fig. 5. Similar plots for a relatively moderately-deep cylindrical panel are presented in Figs 6–9, showing convincing results.

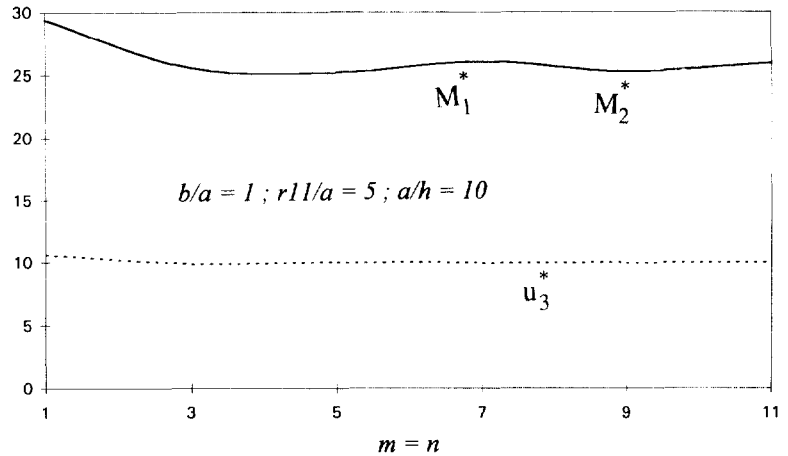

Fig. 2. Convergence of central values of u_3^*, M_1^*, and M_2^* for a cylindrical panel with $(r_{11}/a) = 5$, $(b/a) = 1$, and $(a/h) = 10$.

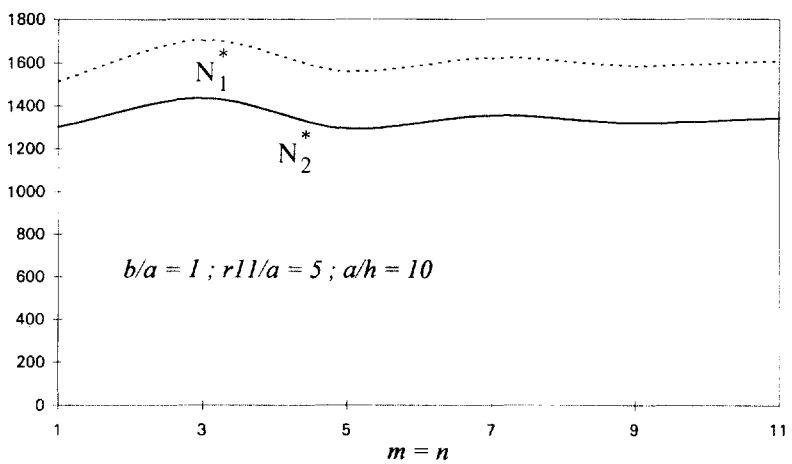

Fig. 3. Convergence of central values of N_1^* and N_2^* for a cylindrical panel with $(r_{11}/a) = 5$, $(b/a) = 1$, and $(a/h) = 10$.

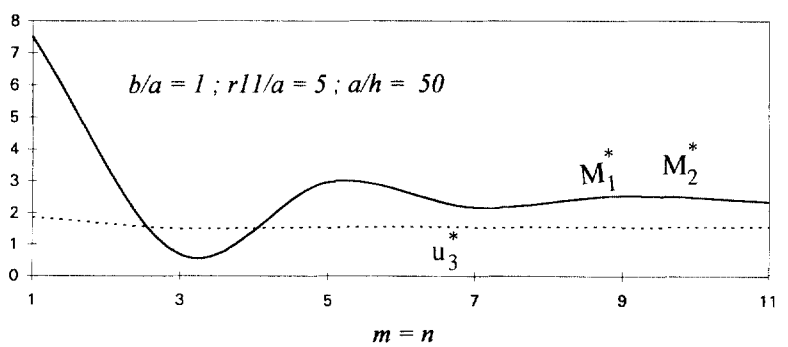

Fig. 4. Convergence of central values of u_3^*, M_1^*, and M_2^* for a cylindrical panel with $(r_{11}/a) = 5$, $(b/a) = 1$, and $(a/h) = 50$.

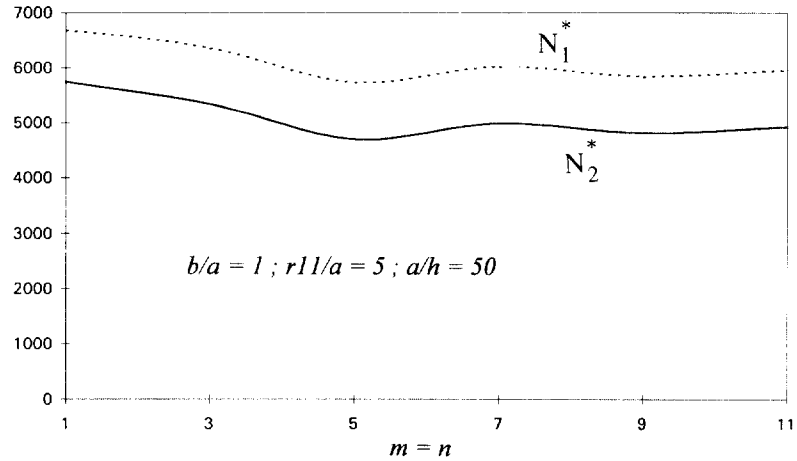

Fig. 5. Convergence of central values of N_1^* and N_2^* for a cylindrical panel with $(r_{11}/a) = 5$, $(b/a) = 1$, and $(a/h) = 10$.

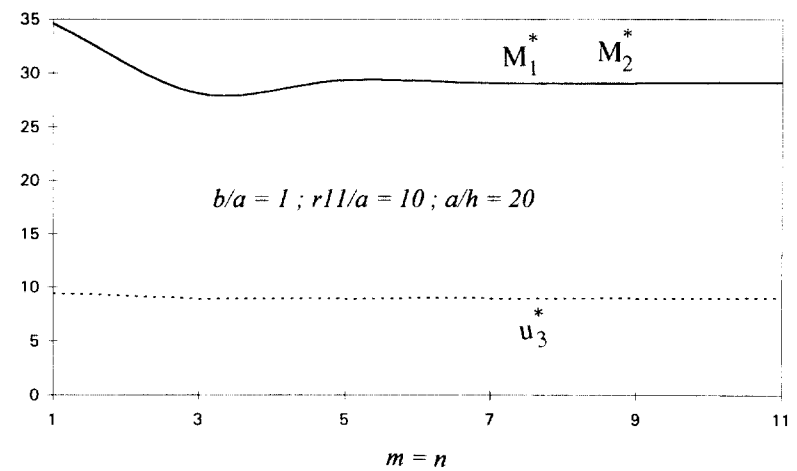

Fig. 6. Convergence of central values of u_3^*, M_1^*, and M_2^* for a cylindrical panel with $(r_{11}/a) = 10$, $(b/a) = 1$, and $(a/h) = 20$.

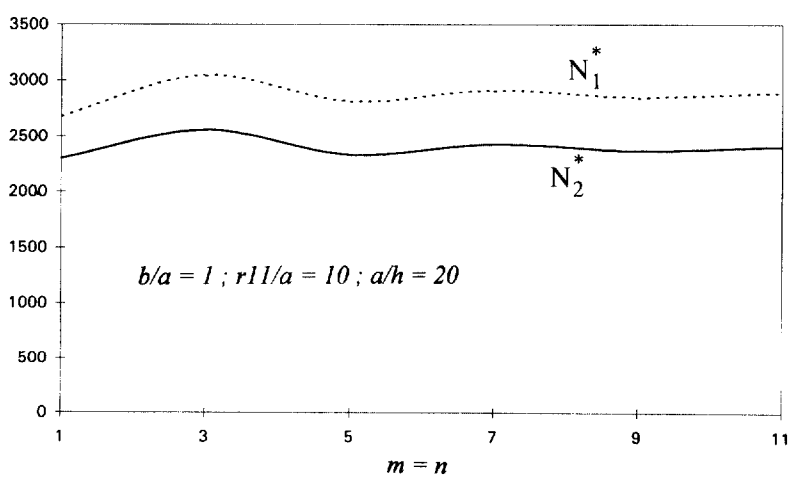

Fig. 7. Convergence of central values of N_1^* and N_2^* for a cylindrical panel with $(r_{11}/a) = 10$, $(b/a) = 1$, and $(a/h) = 20$.

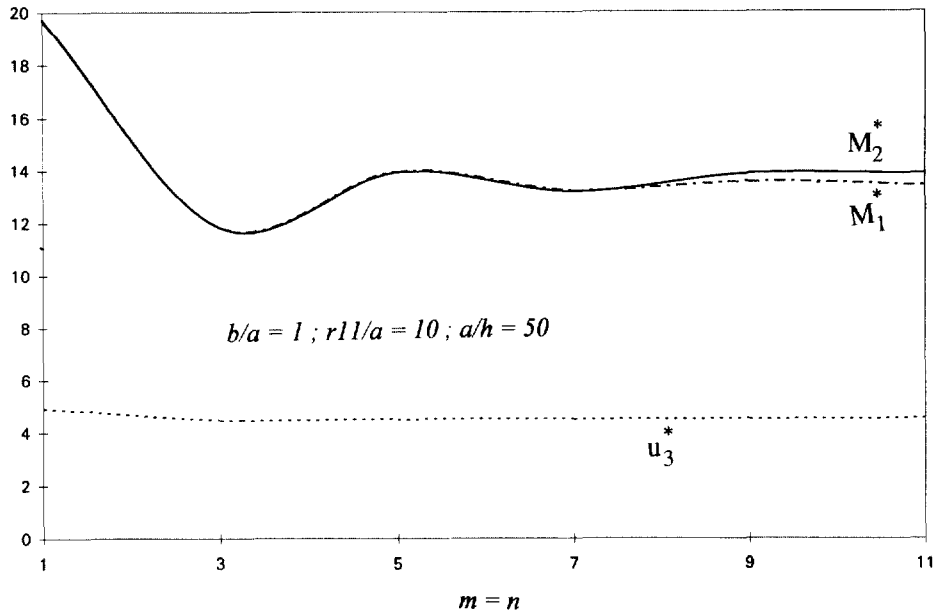

Fig. 8. Convergence of central values of u_3^*, M_1^*, and M_2^* for a cylindrical panel with $(r_{11}/a) = 10$, $(b/a) = 1$, and $(a/h) = 50$.

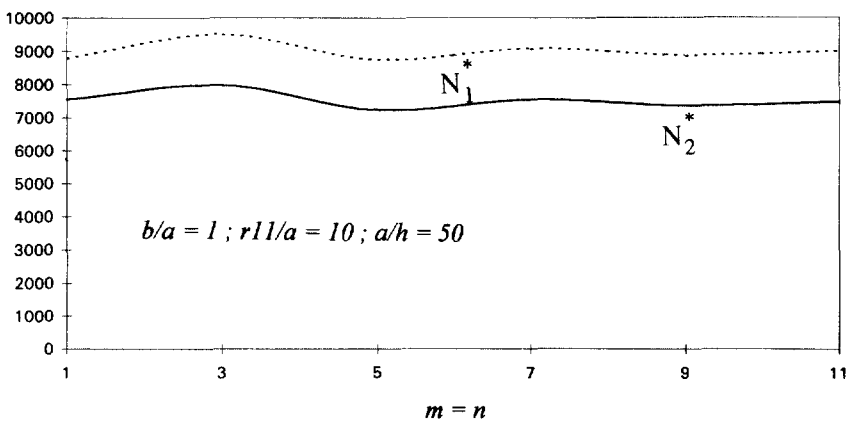

Fig. 9. Convergence of central values of N_1^* and N_2^* for a cylindrical panel with $(r_{11}/a) = 10$, $(b/a) = 1$, and $(a/h) = 50$.

Variations of u_3^*, M_1^*, and M_2^* in Fig. 10, and N_1^*, and N_2^* in Fig. 11 with respect to various a/h for a cylindrical panel having $b/a = 1$, $r_{11}/a = 5$, and $m = n = 9$ are presented. The membrane effect dominates over the flexure as a/h increases. Similar trend is not found for the case of same panel with $r_{11}/a = 50$, a moderately deep situation. The moments remain constant for $a/h \geqslant 20$ (Fig. 12), while the membrane effect dominates with the rise of a/h. Figures 13–17 plot the effects for various a/h of the same panel with $b/a = 5$. In case of moderately shallow panel, moment increases with the increase of a/h, then starts decreasing with $a/h \geqslant 15$.

Variations of u_3^*, M_1^*, and M_2^* with respect to various r_{11}/a are presented in Fig. 18. Variations of them are not distinctive for $r_{11}/a \geqslant 50$. Variations of N_1^*, and N_2^* with respect to various r_{11}/a for the previous panel are given in Fig. 19. The stress resultants, N_1^*, and N_2^* sharply abate with the increase of r_{11}/a.

Spatial variations of N_1^*, N_2^*, M_1^*, and M_2^* are given in a most panoramic way in the form of contour plots in Figs 20–23, respectively, for $b/a = 1$, $a/h = 5$, and $r_{11}/a = 5$.

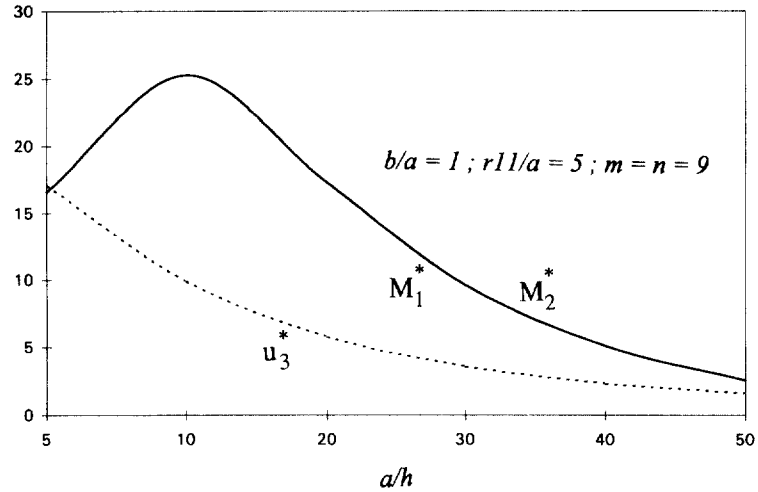

Fig. 10. Variations of central values of u_3^*, M_1^*, and M_2^* with respect to a/h for a cylindrical panel with $(r_{11}/a) = 5$ and $(b/a) = 1$, and $m = n = 9$.

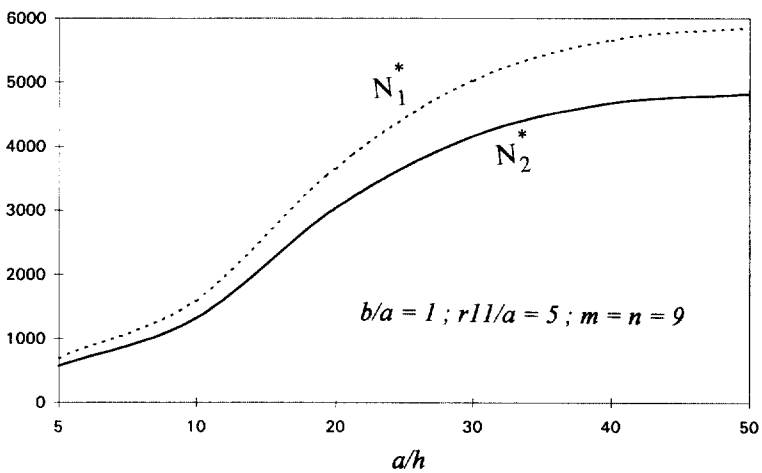

Fig. 11. Variations of central values of N_1^* and N_2^* with respect to a/h for a cylindrical panel with $(r_{11}/a) = 5$ and $(b/a) = 1$, and $m = n = 9$.

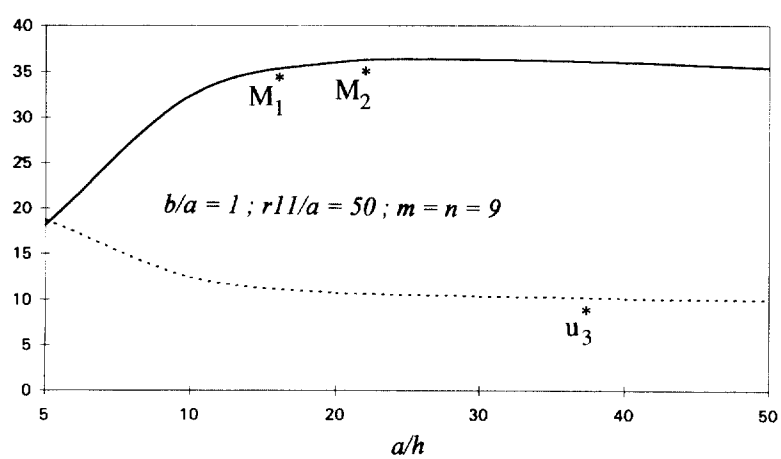

Fig. 12. Variations of central values of u_3^*, M_1^*, and M_2^* with respect to a/h for a cylindrical panel with $(r_{11}/a) = 50$ and $(b/a) = 1$ and $m = n = 9$.

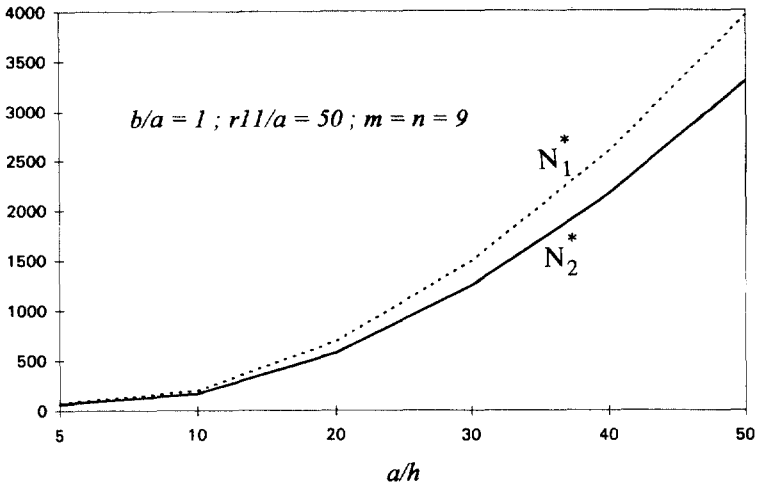

Fig. 13. Variations of central values of N_1^* and N_2^* with respect to a/h for a cylindrical panel with $(r_{11}/a) = 50$ and $(b/a) = 1$, and $m = n = 9$.

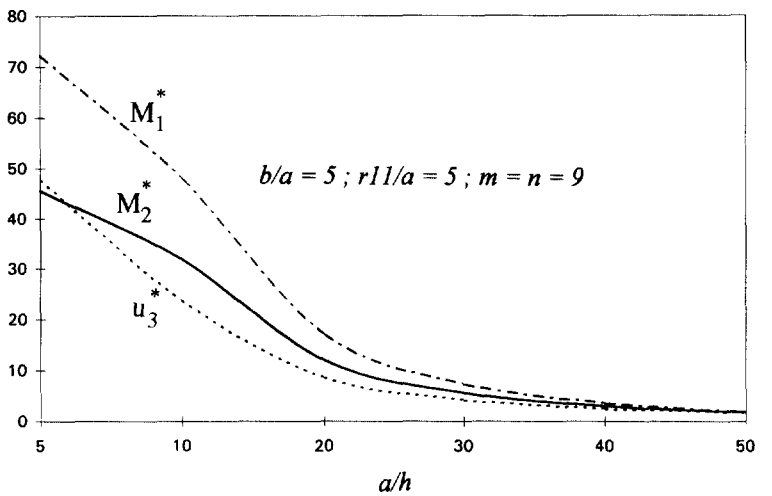

Fig. 14. Variations of central values of u_3^*, M_1^*, and M_2^* with respect to a/h for a cylindrical panel with $(r_{11}/a) = 5$ and $(b/a) = 5$, and $m = n = 9$.

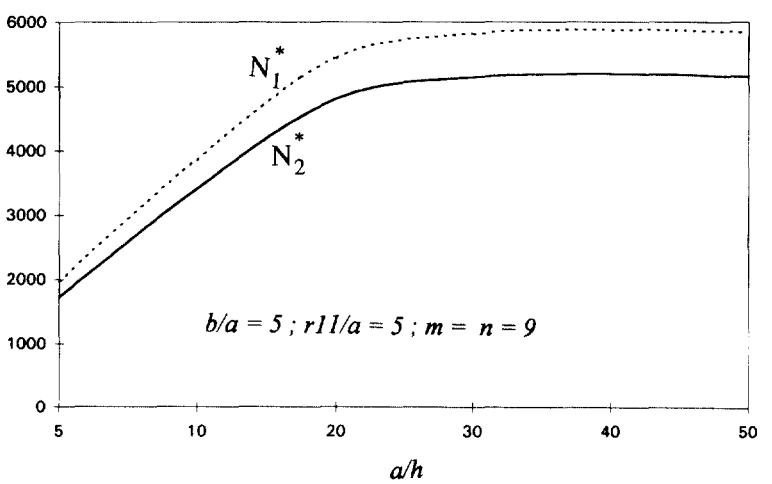

Fig. 15. Variations of central values of N_1^* and N_2^* with respect to a/h for a cylindrical panel with $(r_{11}/a) = 5$ and $(b/a) = 5$, and $m = n = 9$.

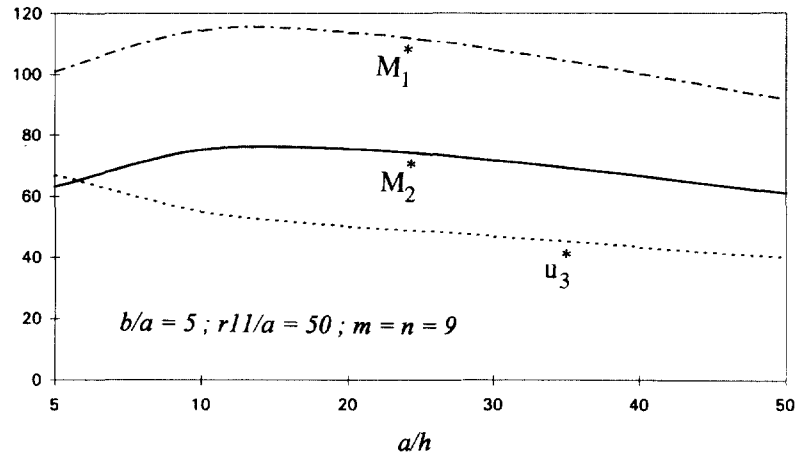

Fig. 16. Variations of central values of u_3^*, M_1^*, and M_2^* with respect to a/h for a cylindrical panel with $(r_{11}/a) = 50$ and $(b/a) = 5$, and $m = n = 9$.

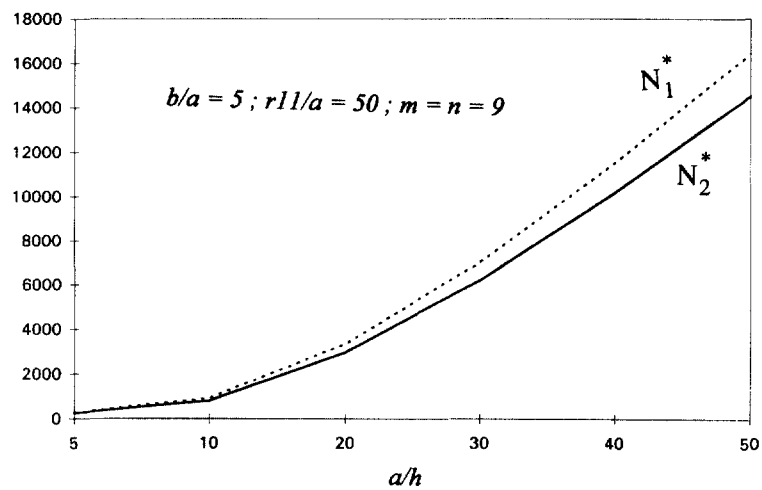

Fig. 17. Variations of central values of N_1^* and N_2^* with respect to a/h for a cylindrical panel with $(r_{11}/a) = 5$ and $(b/a) = 5$, and $m = n = 9$.

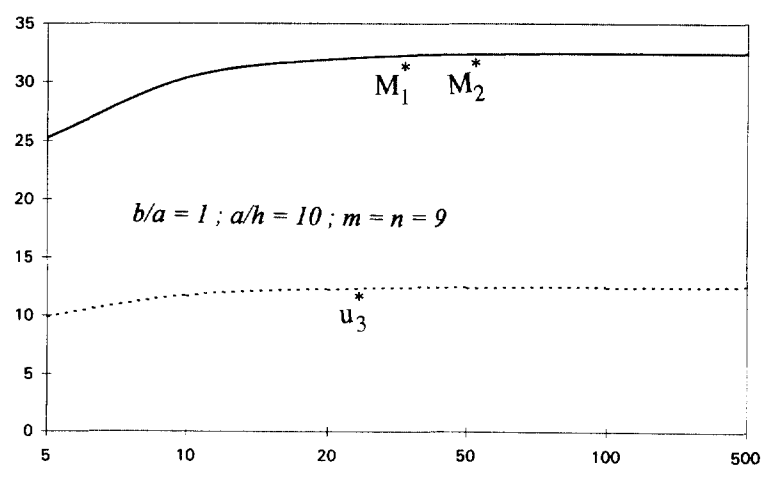

Fig. 18. Variations of central values of u_3^*, M_1^*, and M_2^* with respect to (r_{11}/a) for a cylindrical panel with $(a/h) = 10$ and $(b/a) = 1$, and $m = n = 9$.

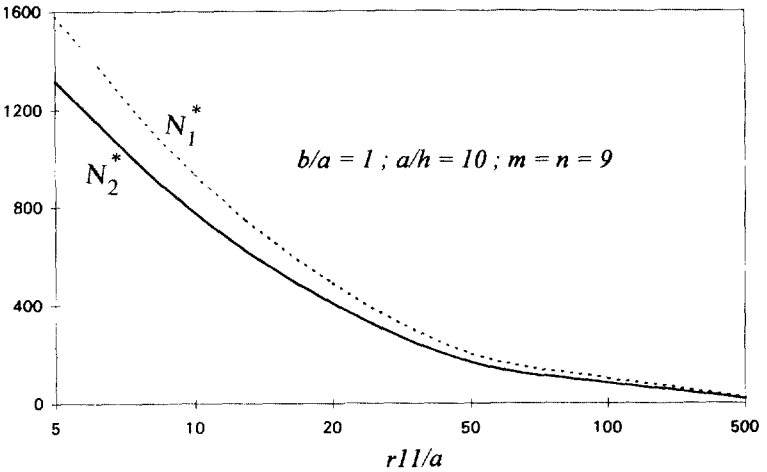

Fig. 19. Variations of central values of N_1^* and N_2^* with respect to (r_{11}/a) for a cylindrical panel with $(a/h) = 10$ and $(b/a) = 1$, and $m = n = 9$.

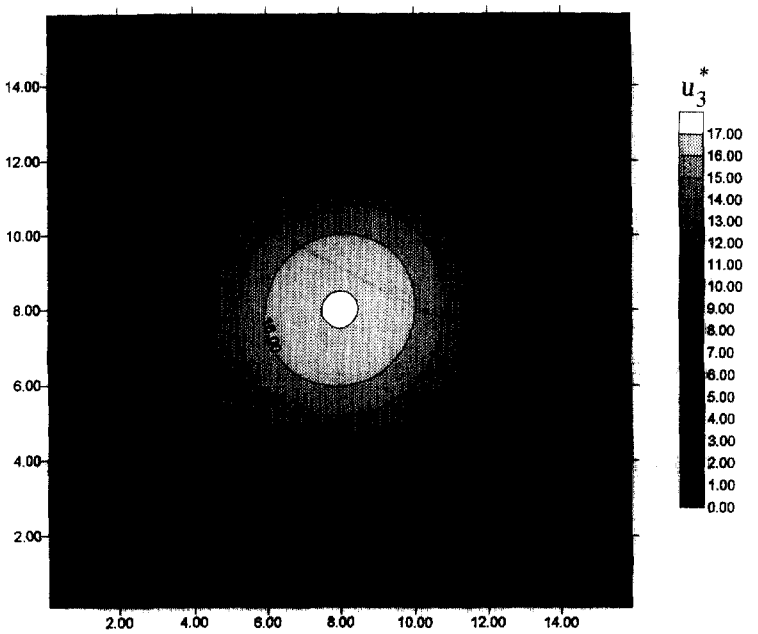

Fig. 20. Contour plotting for spatial variations of N_1^* for a cylindrical panel with $(r_{11}/a) = 5$, $(a/h) = 5$, and $(b/a) = 1$.

The numerical results obtained from the present analysis are compared with the first order shear deformation theory-based finite element formulation, and analytical solution. A four-node quadrilateral finite element according to the work of Bathe and Dvorkin (1984), is considered for the former formulation while a double Fourier series solution is adopted for the later one. This four-node quadrilateral element is implemented in NISA (1992), a commercially available generalized finite element package. A cylindrical panel with $(r_{11}/a) = 10$, and $(b/a) = 1$ is considered for $a/h = 10$. The panel modeled with 16×16 finite elements has shown convergency, and details of which are not reported in this paper for the sake of brevity. The variations of u_3^* and M_2^* measured at $x_2 = (b/2)$ along x_1/a are plotted in Figs 24–26, respectively. In all the cases, RMSDT-based solutions over predict the results in comparison to the present study.

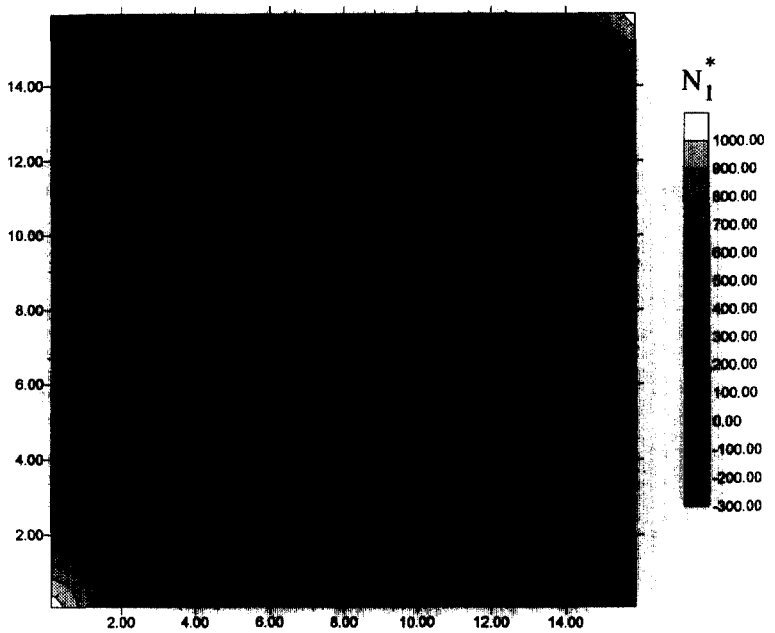

Fig. 21. Contour plotting for spatial variations of N_2^* for a cylindrical panel with $(r_{11}/a) = 5$, $(a/h) = 5$, and $(b/a) = 1$.

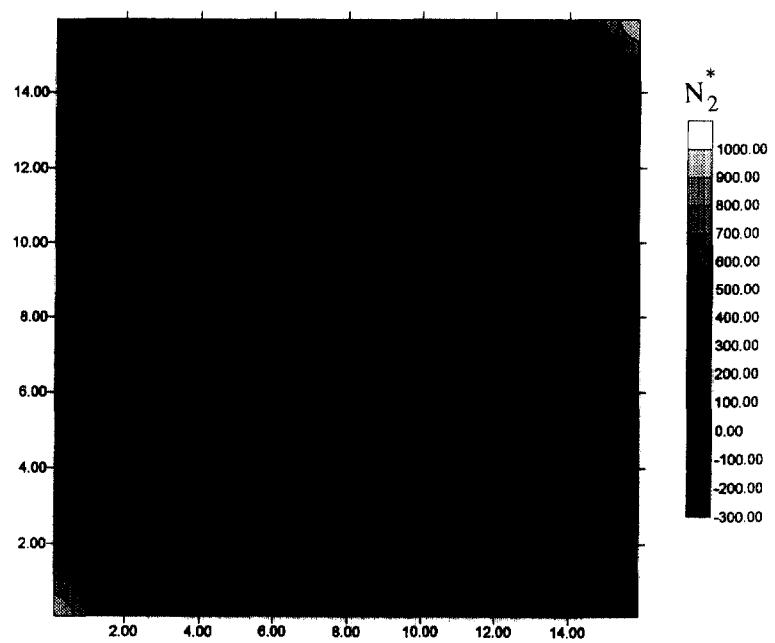

Fig. 22. Contour plotting for spatial variations of M_1^* for a cylindrical panel with $(r_{11}/a) = 5$, $(a/h) = 5$, and $(b/a) = 1$.

CONCLUSIONS

An analytical solution to a boundary-value problem of a thick moderately-deep cylindrical panel with anti-symmetric angle-ply laminations is presented. A boundary continuous solution approach based on double Fourier series solution functions is considered. The numerical results thus presented herein should serve as base line solutions for a future

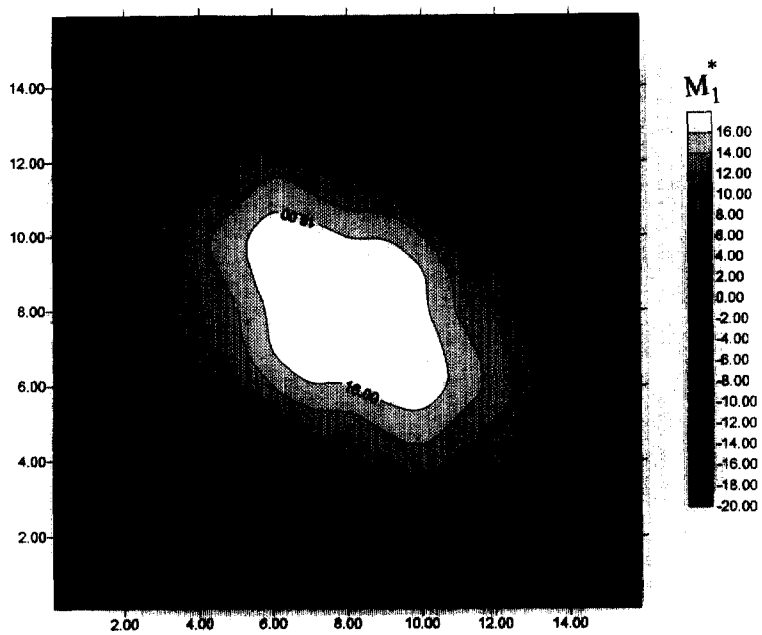

Fig. 23. Contour plotting for spatial variations of M_2^* for a cylindrical panel with $(r_{11}/a) = 5$, $(a/h) = 5$, and $(b/a) = 1$.

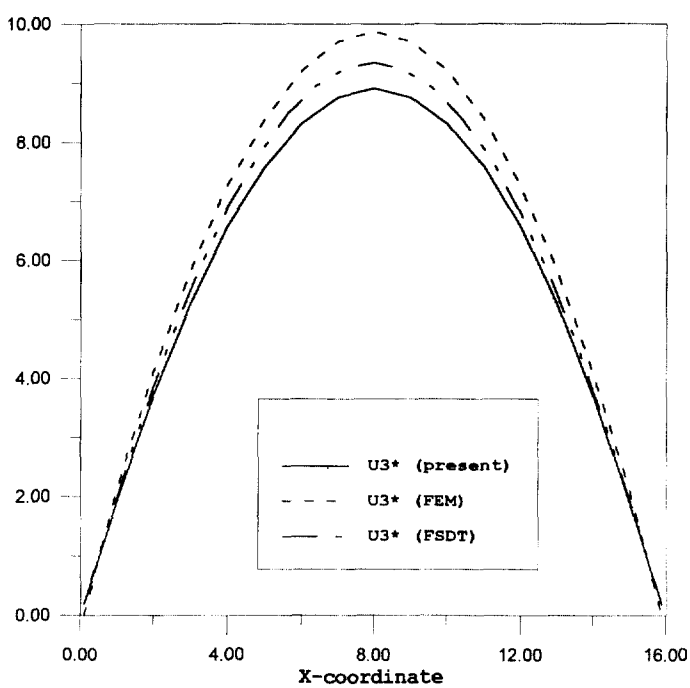

Fig. 24. Comparison of central values of u_3^* obtained using the present solution, RMSDT-based analytical and finite element methods for a cylindrical panel with $(r_{11}/a) = 10$, $(a/h) = 20$, and $(b/a) = 1$.

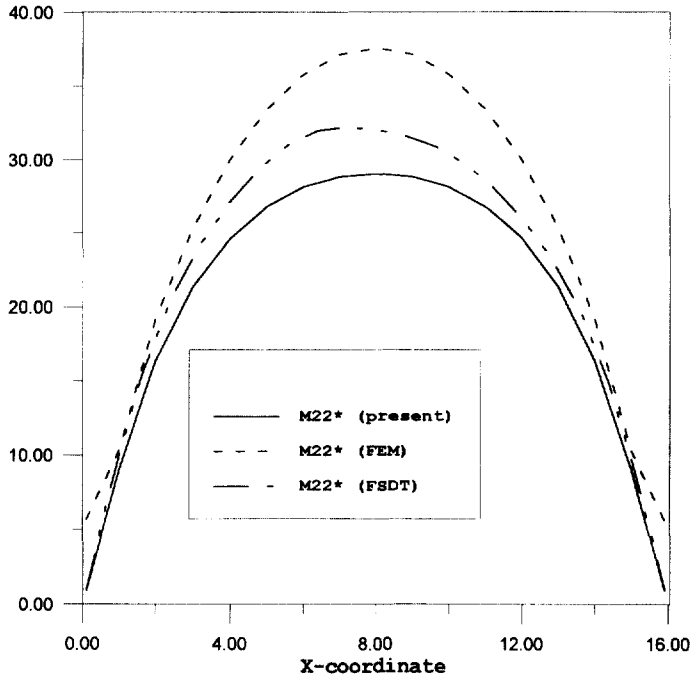

Fig. 25. Comparison of central values of M_1^* obtained using the present solution, RMSDT-based analytical and finite element methods for a cylindrical panel with $(r_{11}/a) = 10$, $(a/h) = 20$, and $(b/a) = 1$.

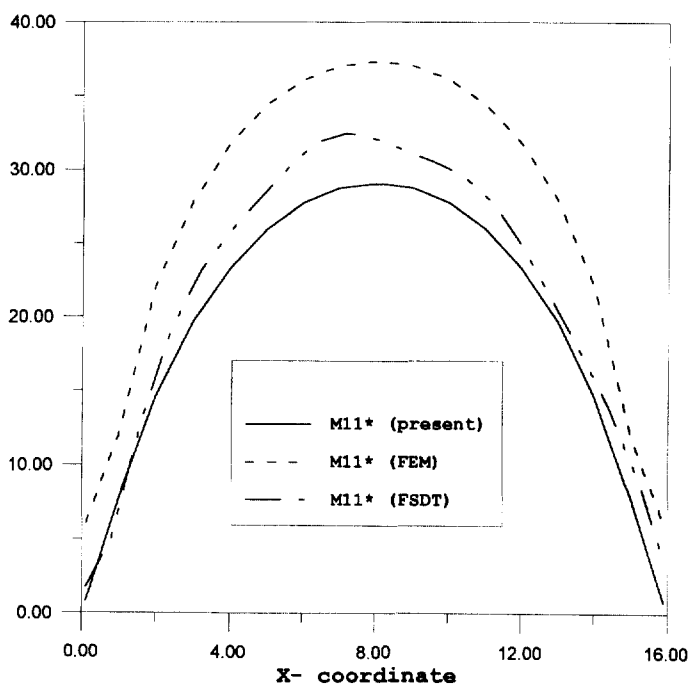

Fig. 26. Comparison of central values of M_2^* obtained using the present solution, RMSDT-based analytical and finite element methods for a cylindrical panel with $(r_{11}/a) = 10$, $(a/h) = 20$, and $(b/a) = 1$.

comparison. The extension of this work to free vibration and buckling problems is under progress.

Acknowledgement—The author wishes to thank Ms Marium and Enrg. Shamsul Haque for their help in obtaining some numerical results, and plotting figures.

REFERENCES

Ambartsumyan, S. A. (1953) Calculation of laminated anisotropic shells. *Izvestiya Akademia Nauk Armenskoi SSR, Seriya Fiziko-Matematicheskikh Estonski Technicheskikh.* **6,** 15.

Andrews, C. (1986) *Elementary Partial Differential Equations with Boundary Value Problems.* Academic Press College Division, New York, U.S.A.

Bathe, K. J. and Dvorkin, E. N. (1985) Short communication—a four node plate bending element based on Mindlin/Reissner plate theory and mixed interpolation. *International Journal of Numerical Methods in Engineering* **21,** 367–383.

Bert, C. W. and Kumar, M. (1982) Vibration of cylindrical shells of bimodulus composite materials. *Journal of Sound Vibration* **81,** 107–121.

Bert, C. W. and Reddy, V. S. (1982) Cylindrical shells of bi-modulus material. *J. Eng. Mech. Div. Am. Soc. Civil Engrs* **81,** 107–121.

Donnell, L. H. (1933) Stability of thin walled tubes in torsion. NACA Report 479.

Flugge, W. (1960) *Stresses in Shells*, 2nd edn. Springer Verlag, Berlin, Germany.

Green, A. E. (1944) Double Fourier series and boundary value problems. *Proc. Camb. Phil. Soc.* **40,** 222–228.

Green, A. E. and Hearmon, R. F. S. (1945) The buckling of flat rectangular plywood plates. *Philosophical Magazine* **36,** 659–687.

Greenberg, J. B. and Stavsky, Y. (1980) Buckling and vibration of orthotropic composite cylindrical shells. *Acta Mechanica* **36,** 15–29.

Hobson, E. W. (1926) *The Theory of Functions of a Real Variable and the Theory of Fourier Series*, Vol. II. Cambridge University Press, Cambridge, U.K.

Hoff, J. N. and Rehfield, L. W. (1965) Buckling of axially cylindrical shells at stresses smaller than the classical critical value. *Journal of Applied Mechanics, ASME* **32,** 542–546.

Jones, R. M. and Morgan, H. S. (1975) Buckling and vibration of cross-ply laminated circular cylindrical shells. *American Institute of Aeronautics and Astronautics Journal* **13,** 664–671.

Kabir, H. R. H. (1994) Analysis of simply supported plate with symmetric angle-ply laminations. *Computers and Structures* **51,** 299–307.

Kabir, H. R. H. and Chaudhuri, R. A. (1991) Free vibration of shear flexible anti-symmetric angle-ply laminated doubly curved panels. *International Journal of Solids and Structures* **28,** 17–32.

Kabir, H. R. H. and Chaudhuri, R. A. (1994) On Gibb's-phenomenon-free Fourier solution for finite shear-flexible laminated clamped panels. *Int. J. Engng. Sci.* **32,** 501–521.

Librescu, L., Khdeir, A. A. and Fredderick, D. (1989) A shear deformable theory of laminated composite shallow shell-type panels and their response analysis I: free vibration and buckling. *Acta Mechanica* **76,** 1–12.

Levinson, M. (1980) An accurate simple theory of the statics and dynamics of elastic plates. *Mechanics Research Communication* **7,** 343–450.

Lo, K. H., Cristensen, R. M. and Wu, E. M. (1977a) A higher-order theory of plate deformation. Part I, Homogeneous plates. *Journal of Applied Mechanics* **44,** 663–668.

Lo, K. H., Cristensen, R. M. and Wu, E. M. (1977b) A higher-order theory of plate deformation. Part II, Laminated plates plate. *Journal of Applied Mechanics* **44,** 669–676.

McElman, J. A. and Knoll, A. C. Jr. (1971) Vibration and buckling analysis of composite plates and shells, *Journal of Composite Materials* **5,** 529–532.

Mindlin, R. D. (1951) Influence of rotatory inertia and shear on flexural motion of isotropic elastic plates. *Journal of Applied Mechanics* **18,** 31–38.

Murthy, M. V. V. (1981) An improved transverse shear deformation theory for laminated anisotropic plates. NASA Technical Paper 1903.

Nelson, R. B. and Lorch, D. R. (1974) A refined theory for laminated orthotropic plates. *Journal of Applied Mechanics* **44,** 177–183.

NISA-II (1992) Engineering Mechanics Research Corporation, Troy, Michigan, U.S.A.

Reddy, J. N. and Liu, C. F. (1985) A higher order shear deformation theory of laminated elastic shells. *Int. J. Engng. Sci.* **23,** 319–330.

Reddy, J. N. and Robbins, Jr D. H. (1994) Theories and computational models for composite laminates. *Applied Mechanics Review* **47,** 147–169.

Reissner, E. (1944) On the theory of bending of elastic plates. *J. Math. Phy.* **23,** 184–191.

Seide, P. (1975) *Small Elastic Deformations of Thin Shells.* Noordhoff International Publishing, Leyden, The Netherlands.

Soldatos, K. P. (1984) A comparison of some shell theories used for the dynamic analysis of cross-ply laminated circular panels. *Journal of Sound Vibration* **97,** 305–319.

Soldatos, K. P. and Tzivandidis, G. J. (1982) Buckling and Vibration of cross-ply laminated circular cylindrical panels. *Journal of Applied Mathematics and Physics (ZAMP)* **33,** 230–239.

Stavsky, Y. and Lowey, R. (1971) On vibrations of heterogeneous orthotropic cylindrical shells. *Journal of Sound Vibration* **15,** 235–256.

Whitney, J. M. (1970) The effect of boundary conditions at the response of laminated composites. *Journal of Composite Materials* **4,** 192–203.

Whitney, J. M. and Leissa, A. W. (1969) Analysis of heterogeneous anisotropic plates. *ASME Journal of Applied Mechanics* **36,** 261–266.

APPENDIX 1

For the sake of brevity terms related to eqn (23) for $i = 1$ are presented:

$$b_{31}^1 = -\bar{r}_{11}{}^{00}A^{1111}; \quad c_{111}^1 = k_h^{102}A^{1111}; \quad c_{112}^1 = 2^{00}A^{1112}; \quad c_{122}^1 = 2^{00}A^{1122}$$

$$c_{211}^1 = {}^{00}A^{1211}; \quad c_{212}^1 = {}^{00}A^{1212} + {}^{00}A^{11211}; \quad c_{222}^1 = {}^{00}A^{1222}$$

$$c_{211}^1 = {}^{00}A^{1211}; \quad c_{212}^1 = {}^{00}A^{1212} + {}^{00}A^{11211}; \quad c_{222}^1 = {}^{00}A^{1222}$$

$$c_{411}^1 = {}^{01}A^{1111} + k_h^{102}A^{1111}; \quad c_{412}^1 = 2^{01}A^{1112} + 2k_h^{102}A^{1112}$$

$$c_{422}^1 = k_h^{102}A^{1122} + {}^{01}A^{1122}; \quad c_{511}^1 = {}^{01}A^{1112} + k_h^{102}A^{1112}$$

$$c_{512}^1 = {}^{01}A^{1122} + {}^{01}A^{1112} + k_h^{102}A^{1112} + k_h^{102}A^{1122}$$

$$c_{522}^1 = {}^{01}A^{1212} + k_h^{102}A^{1212}$$

APPENDIX 2

Definitions of stiffnesses as shown in Appendix 1:

$$\begin{Bmatrix} {}^{00}A^{\alpha\beta;\eta} \\ {}^{01}A^{\alpha\beta;\eta} \\ {}^{11}A^{\alpha\beta;\eta} \\ {}^{02}A^{\alpha\beta;\eta} \\ {}^{12}A^{\alpha\beta;\eta} \\ {}^{22}A^{\alpha\beta;\eta} \end{Bmatrix} = \sum_{k=1}^{N} \left(E_{\langle k\rangle}^{\alpha\beta;\eta} - \frac{E_{\langle k\rangle}^{\alpha\beta 33} E_{\langle k\rangle}^{33;\eta}}{E_{\langle k\rangle}^{3333}} \right) \begin{Bmatrix} t_{\langle k\rangle} - t_{\langle k-1\rangle} \\ \frac{1}{2}(t_{\langle k\rangle}^2 - t_{\langle k-1\rangle}^2) \\ \frac{1}{3}(t_{\langle k\rangle}^3 - t_{\langle k-1\rangle}^3) \\ \frac{1}{4}(t_{\langle k\rangle}^4 - t_{\langle k-1\rangle}^4) \\ \frac{1}{5}(t_{\langle k\rangle}^5 - t_{\langle k-1\rangle}^5) \\ \frac{1}{7}(t_{\langle k\rangle}^7 - t_{\langle k-1\rangle}^7) \end{Bmatrix} \tag{2.1}$$

$$\begin{aligned} {}^{00}A^{\alpha 3;3} &= \sum_{k=1}^{N} E_{\langle k\rangle}^{\alpha\beta 33}(t_{\langle k\rangle} - t_{\langle k-1\rangle}) \\ {}^{11}A^{\alpha 3;3} &= \sum_{k=1}^{N} E_{\langle k\rangle}^{\alpha\beta 33}\frac{1}{3}(t_{\langle k\rangle}^3 - t_{\langle k-1\rangle}^3) \\ {}^{12}A^{\alpha 3;3} &= \sum_{k=1}^{N} E_{\langle k\rangle}^{\alpha\beta 33}\frac{1}{5}(t_{\langle k\rangle}^5 - t_{\langle k-1\rangle}^5) \end{aligned} \tag{2.2}$$

APPENDIX 3

Definitions of unknown constants arising in eqn (29):

$$g_{m(1)}^{3111} = \frac{4}{ab}\int_0^b \{v_{3,11}(a, x^2) - u_{3,11}(0, x^2)\} \sin(\beta_n x^2)\, \mathrm{d}x^2$$

$$g_{m(2)}^{3111} = -\frac{4}{ab}\int_0^b \{u_{3,11}(a, x^2) + u_{3,11}(0, x^2)\} \sin(\beta_n x^2)\, \mathrm{d}x^2$$